Investigation on P-N dual acceptor doped p-type ZnO thin films and subsequent growth of pencil-like nanowires

2015 Semicond. Sci. Technol. 30 035009

(http://iopscience.iop.org/0268-1242/30/3/035009)

IOP Publishing Semiconductor Science and Technology
Semicond. Sci. Technol. **30** (2015) 035009 (10pp) doi:10.1088/0268-1242/30/3/035009

Investigation on P-N dual acceptor doped p-type ZnO thin films and subsequent growth of pencil-like nanowires

R Amiruddin, Sebin Devasia, D K Mohammedali and M C Santhosh Kumar

Optoelctronic Materials and Devices Lab, Department of Physics, National Institute of Technology, Tiruchirappalli-620 015, India

E-mail: amirphy9@yahoo.com and santhoshmc@nitt.edu

Received 7 October 2014, revised 17 December 2014
Accepted for publication 18 December 2014
Published 13 January 2015

Abstract

Phosphorous and nitrogen dual acceptor doped p-type ZnO (PNZO) have been deposited by spray pyrolysis method on glass substrates. An equimolar doping concentration of P and N were varied from 0.25–1.25 at% with a step of 0.25 at%. Preferred orientation along (002) planes with hexagonal wurzite structure was observed from structural analysis. Morphological analysis reveals uniform distributions of grains. Electrical studies showed dual acceptor doping of P and N in ZnO results in p-type behavior. The optimum doping concentration of P and N was found to be 0.75 at% which exhibited hole concentration of 4.48×10^{18} cm^{-3} and low resistivity value of 9.6 Ω.cm. Photoluminescence (PL) studies revealed that, as-deposited films exhibit strong UV emission at 383 nm of the spectrum. The surface morphology of the optimum PNZO (0.75 at%) samples were further modified in the form of vertically aligned pencil-like nanowires by modified aqueous chemical growth (ACG) process. During ACG process, more acceptor related defects such as oxygen interstitials (O_i) were formed in the PNZO nanopencils. These acceptor defects induce enhanced emission in the visible region (400 nm to 700 nm) and also promote stable p-type characteristics.

Keywords: dual acceptor doping, p-type ZnO, aqueous chemical growth (ACG), pencil-like nanowires

(Some figures may appear in colour only in the online journal)

1. Introduction

In recent years, ZnO has gained considerable attention as a potential material for optoelectronic applications such as light emitting diodes (LEDs) [1], LASERS [2] and solar cells [3]. Successful growth of p-type ZnO and fabrication of p-n junctions are considered as crucial steps to realize these applications. ZnO being an intrinsic n-type semiconductor possesses unique properties such as low cost, wide band gap (3.36 eV) and large exciton binding energy (60 meV) [4]. However, difficulty arises in achieving stable p-type ZnO due to the presence of predominant native defects such as zinc interestials (Zn_i) and oxygen vacancy (V_o). These defects act as native electron donors which compensate the formation of p-type behavior in ZnO [5]. This self-compensation effect is considered as the major difficulty in achieving stable p-type ZnO. The other reasons include the presence of deep acceptor levels and low solubility of the dopants which acts as a barrier for successful realization of p-type ZnO. In spite of native n-type characteristics, many efforts have been made to grow good quality p-type ZnO layers, and remarkable progress has been made both theoretically and experimentally [6, 7]. Nevertheless, the stability and reproducibility in achieving p-type ZnO remains unsolved. Some notable attempts in realization of p-type ZnO include doping of Group-I (Li, Na and K) and Group-V (P, N and Sb) elements in ZnO [8]. However, in the majority of cases, monodoping of these acceptor elements in ZnO is considered to possess poor reproducibility. It is believed that monodoping effect results in deep acceptor levels and possesses low holes concentration which

lacks the ability to compensate the intrinsic native donor defects. Other efforts include co-doping method [9] to overcome the hindrances in achieving p-type conductivity in ZnO thin films. Co-doping method was theoretically predicted by Yamamoto and Yoshid for the realization of p-type ZnO films [10]. In this method, the acceptor (N) atoms and donor atoms (like Al, Ga and In) with a ratio of 2:1 are doped simultaneously in ZnO. This results in formation of acceptor-donor-acceptor complexes which play the key role in formation of p-type ZnO films by co-doping method. However, due to the presence of donor atoms, co-doping method may also result in self-compensation effect. An alternative method for realization of p-type ZnO includes dual acceptor doping effect introduced by Krtschil *et al* [11]. Since both the doping elements possess acceptor properties, self-compensation can be controlled and it also helps in sustaining higher holes concentration [12–14].

In the present work, dual acceptor group-V elements such as P and N are simultaneously doped in ZnO films to obtain the p-type characteristics. As a result of the ACG process, the surface morphology of PNZO films was modified in the form of vertically aligned one-dimensional p-type ZnO nanostructures. The structural, morphological, electrical and luminescence properties were investigated. The optimum PNZO nanostructures are found to possess more acceptor defects such as oxygen interstitials (O_i) by aqueous chemical growth process.

2. Experimental

In order to deposit p-type ZnO seed layers, we have adopted the spray pyrolysis method due to its simplicity and cost effectiveness in preparing good quality of thin films under non-vacuum condition. 0.1 M concentration of precursor solution is prepared by dissolving zinc acetate dehydrate (Sigma-Aldrich, 99.5%, Germany) in a solvent mixture containing 10 ml of ethanol and 90 ml deionized water. In order to make the prepared solution homogenous and transparent, 3 ml of acetic acid is added. Di-phosphorous pentaoxide (Merck, extra pure, 99.9%, Germany) and ammonium acetate (Sigma-Aldrich, 99.5%, Germany) were used as a dopant sources for phosphorous and nitrogen, respectively. An equimolar doping ratio of P and N is varied ranging from 0.25–1.25 at% with a step of 0.25 at%. Finally, the prepared precursor solution is sprayed uniformly upon soda lime glass substrates. The glass substrates were ultrasonically cleaned for 30 min before depositing the films. The films were deposited by programmable and automated spray pyrolysis (HOLMARC, India) set up. A schematic illustration of the programmable spray pyrolysis set up and the optimized deposition parameters can be found elsewhere [15]. The as-deposited thin film samples are coded as PNZO (0.25), PNZO (0.50), PNZO (0.75), PNZO (1.0), and PNZO (1.25). The deposited films were later used as a seed layer in aqueous chemical growth (ACG) process in order to modify the surface in the form of vertically aligned one-dimensional nanostructures.

For the fabrication of one-dimensional nanostructures, the optimum PNZO (0.75) samples were subjected to the ACG process [16]. In this case, the precursor solution was prepared by dissolving equimolar concentration of 0.01 M zinc nitrate ($Zn(NO_3)_2.6H_2O$) and hexa methylene tetramine (HMT, $C_6H_{12}N_4$) in de-ionized water. In our earlier report [15], to retain the conductivity of the grown Al doped ZnO nanowires, we have introduced a modified approach in which the optimum dopant concentration was additionally doped during the ACG process. With a similar appeal, in order to retain the p-type characteristics and also to enhance the emission property in the visible region, a modified ACG approach is processed. During the ACG process, the optimum doping concentrations of P and N (0.75 at%) were also doped along with the zinc nitrate by adding appropriate quantities of di-phosphorous pentaoxide and ammonium acetate. The PNZO (0.75) seed layer is dipped horizontally in the prepared aqueous solution mixture. The dipping duration is 5 h while maintaining the temperature at 90 °C. After the ACG process, the samples are rinsed thoroughly with de-ionized water to remove additional sediment formation upon the surface and finally dried in air.

The structural analysis was carried out by x-ray diffractometer (RIGAKU ULTIMA III) using CuKα radiation ($\alpha = 1.5406$ Å). The thickness of the seed layer films was measured using a stylus profilometer and it was found to be 800 nm. The vertically aligned PNZO nanostructures show an increased thickness of 1300 nm. The surface morphology of the films was recorded by a field emission scanning electron microscope (FESEM-HITACHI SU6600). The optical measurements of PNZO seed layers and nanostructures were carried out at room temperature using a JASCO V-670 Uv-Vis-NIR spectrophotometer in the wavelength range 300–1100 nm. The electrical resistivity, mobility, carrier concentration and the carrier type of the semiconductor thin films were investigated using Hall measurement (ECOPIA-HMS 5000). Photoluminescence (PL) properties of the films were investigated at room temperature using a JASCO Spectrofluorometer (FP 8500) with an excitation wavelength of 325 nm.

3. Results and discussion

3.1. Morphological studies

Figures 1(a)–(c) depicts the SEM images of PNZO (0.25), PNZO (0.75) and PNZO (1.25) seed layers. It is perceived that uniform grains are distributed throughout the surface. Figure 1(d) shows the EDAX spectrum of PNZO (0.75) films. The presence of main elements such as Zn, O, P and N were confirmed from the EDAX analysis. The optimum concentration of PNZO seed layer was subjected to the ACG process for growth of vertically aligned nanostructures. From SEM analysis, it is revealed that the vertically aligned nanowires consist of sharp edges resembling sharpened pencils. Figure 2 shows the SEM images of (a) PNZO (0.75) nanopencils (top view) and (b) 30° tilted view of the grown

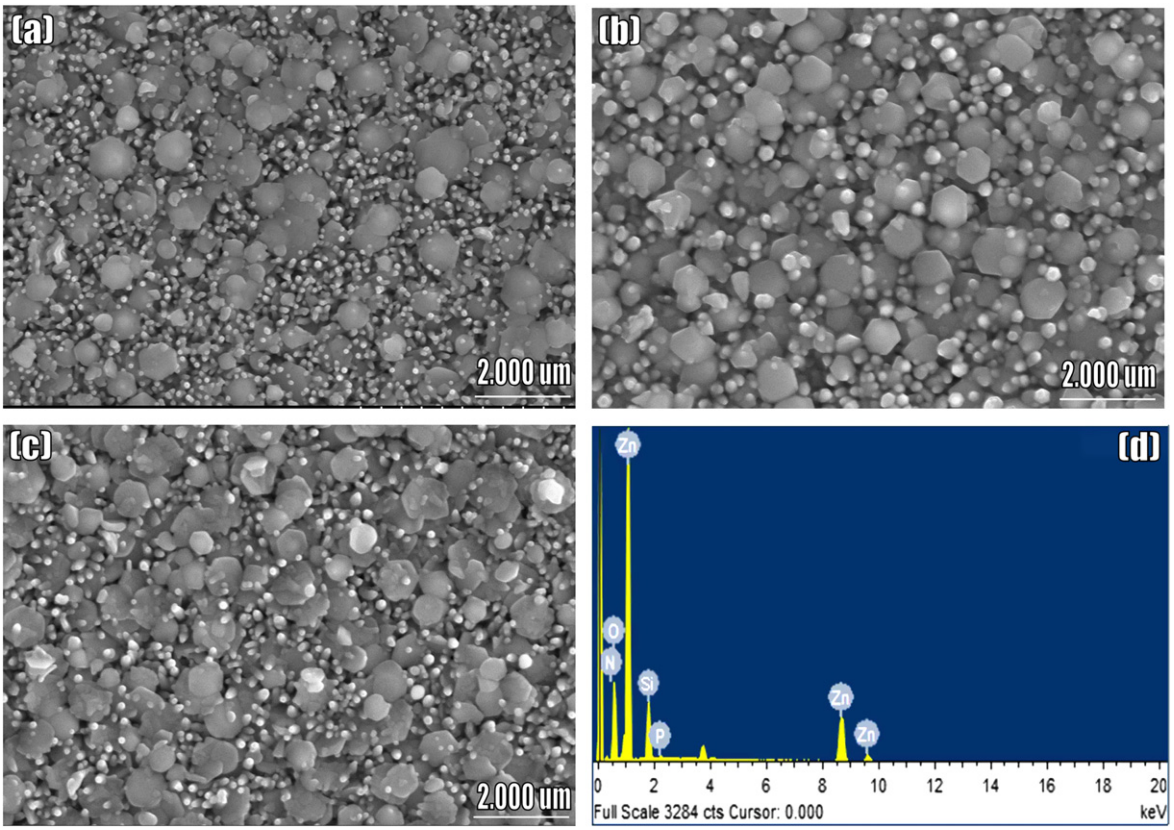

Figure 1. SEM images of (a) PNZO (0.25 at%) (b) PNZO (0.75 at%) (c) PNZO (1.25 at%) seed layers and (d) EDAX spectrum of the PNZO (0.75 at%) films.

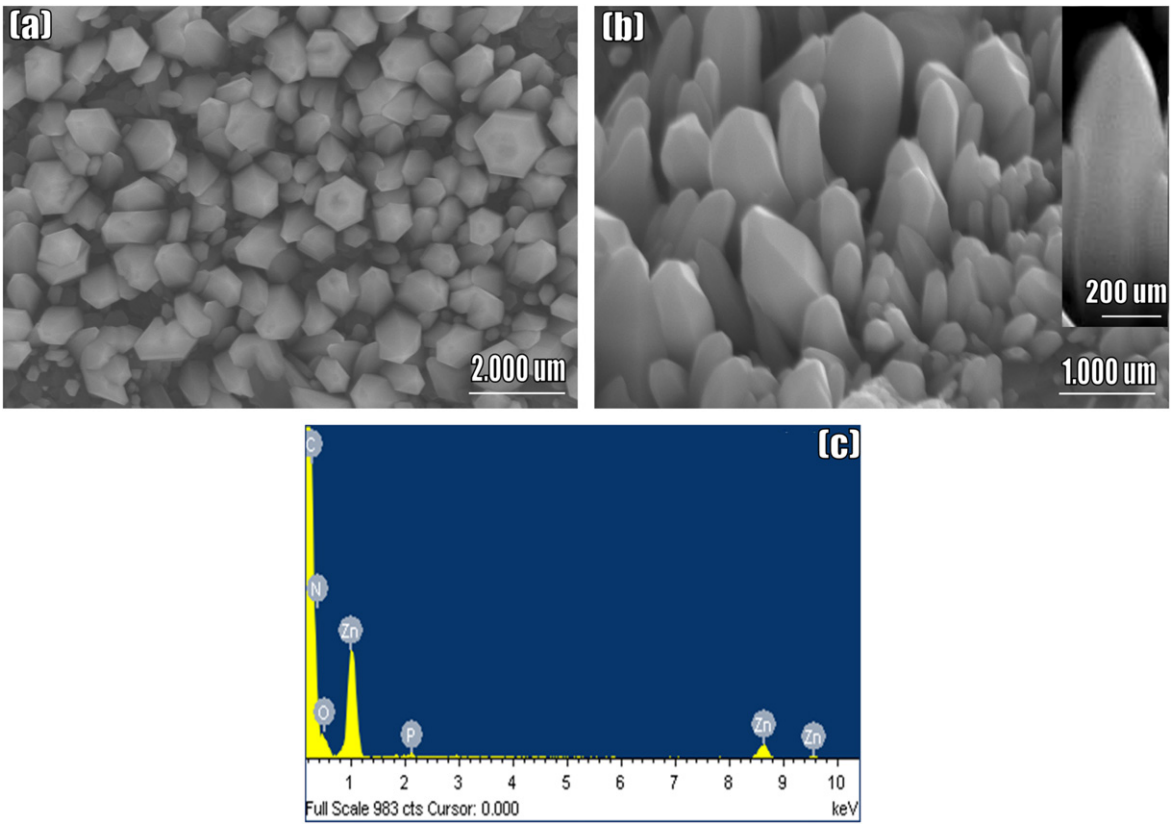

Figure 2. SEM images of (a) top view, (b) tilted 30° view of PNZO (0.75 at%) nanopencils and (c) EDAX spectrum of the PNZO (0.75 at%) nanopencils.

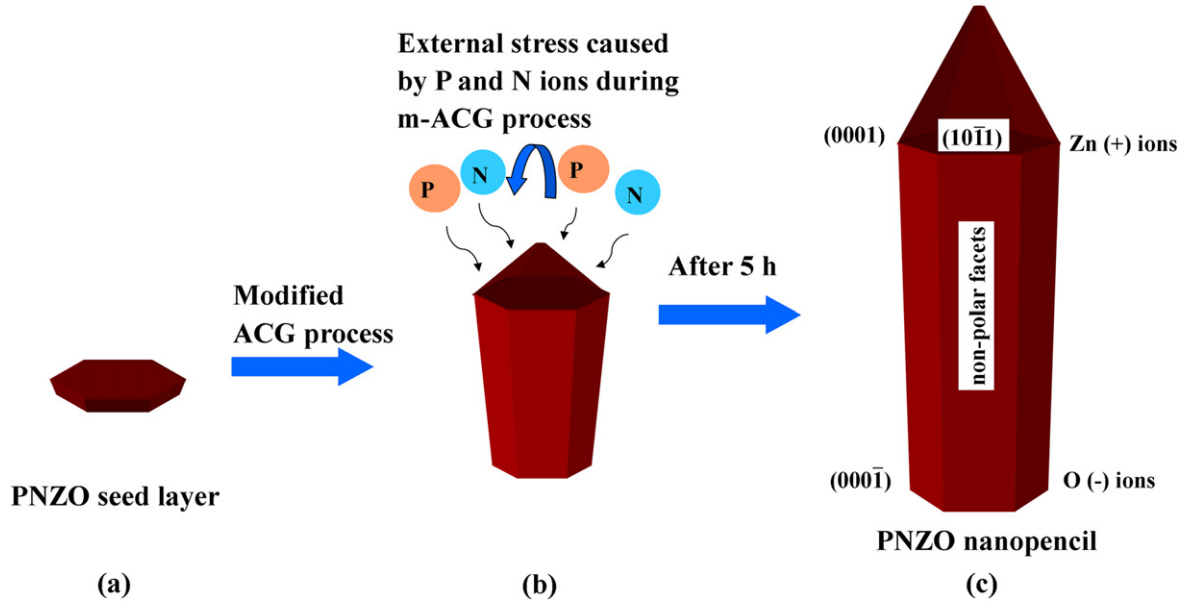

Figure 3. Shows the schematic illustration (a) as deposited PNZO (0.75 at%) seed layers, (b) the formation of PNZO pencil-like nanowires (with sharp edges) due to external stress caused by phosphorous and nitrogen dopant atoms during modified aqueous chemical growth process and (c) the final product of as-grown PNZO nanopencils after 5 h of modified ACG process.

PNZO (0.75) nanopencils. The formation of pencil-like nanowires by modified ACG process was not observed in our earlier report [15], for the growth of Al doped conducting ZnO nanowires. The growth mechanism for the observed PNZO (0.75) pencil-like nanowires can be understood on the basis of crystallographic arrangement of hexagonal ZnO [17]. The wurtzite structure of ZnO can be illustrated as a number of alternating planes composed of tetrahedrally coordinated O^{2-} and Zn^{2+} ions stacked alternately along the c-axis [18]. ZnO possesses weak polar characteristics where one end of the basal polar plane terminates with partially positive Zn lattice sites (0001) and the other end terminates in partially negative oxygen lattice sites $(000\bar{1})$. This results in spontaneous polarization along the c-axis and consequently variation in surface energies takes place between polar and non-polar facets of ZnO [18]. The surface energy of polar facets of ZnO is twice that of non-polar facets. This makes the polar facets become unstable and growth along this direction becomes higher than with non-polar facets [19]. When PNZO (0.75) seed layers are subjected to the ACG process, the growth rate will be higher for Zn terminated polar facets (0001) and lower for non-polar facets and the least for the O terminated polar facets $(000\bar{1})$ [20]. During the ACG process, flat crystal faces of ZnO tend to appear and this results in vertical growth along c-axis. The bonding between Zn and O stretches along the c-axis (faces) and at the same time contracts perpendicular to c-axis (walls of nanowires). One of the key criteria in tailoring the morphology of the one-dimensional ZnO nanostructures is to tune the surface energy of the different facets in ZnO. Apart from (0001) polar faces, ZnO possess other typical polar facets: $(10\bar{1}1)$ which is considered a key factor for formation of sharp edges at the tip of the grown nanostructures. The $(10\bar{1}1)$ polar facets possess higher Miller index and low surface energy in comparison to (0001) polar faces. The growth path of the ZnO nanostructures can be controlled by their growth kinetics, doping or by carbothermal reduction process. There are notable reports in tuning the surface energy of $(10\bar{1}1)$ polar facets of ZnO that leads to the formation of ZnO nanowires with sharp edges. Zhou *et al* reported the growth of ZnO nanopyramids (pencil-like) by assistance of a passivating agent such as ionic liquid [21]. Ahsanulhaq *et al* [17] reported pencil -like nanowires by increasing the reaction temperature to 110 °C during aqueous chemical growth process.

In the present study, we demonstrate that due to external stress caused by higher ionic radii of doping elements in modified aqueous chemical growth process [15], it is possible to pattern the as-grown nanowires in the form of vertically aligned nanopencils. When these acceptor atoms are intentionally doped during the modified ACG process, it is expected to promote external stress upon the surface of the grown PNZO nanowires. This induces electrostatic interaction between the acceptor ions and the polar surfaces. At this juncture, the polar plane $(10\bar{1}1)$ with higher Miller index and low surface energy is preferred for the further growth process. A sequential 60° tilt angle in growth direction among the six equivalent polar planes $(10\bar{1}1)$ results in formation of nanowires with sharp edges [22]. Figure 2 shows the SEM images of (a) top view and (b) tilted 30° view of PNZO (0.75) nanopencils. Figure 2(c) shows the EDAX analysis of PNZO (0.75) pencil-like nanowires to confirm the presence of elements such as Zn, O, P and N. The average lengths of grown PNZO (0.75) nanowires were found to be 1300 nm. The body portion of the pencil-like nanowires possesses an average diameter of 155 nm. Figure 3 shows the schematic illustration (a) spray deposited PNZO (0.75) seed layers, (b) the formation of PNZO pencil-like nanowires (with sharp edges) due to external stress caused by phosphorous and nitrogen dopant

Table 1. The electrical properties of undoped ZnO films, PNZO (0.25–1.25 at%) seed layers and PNZO (0.75 at%) nanopencils.

Sample	Carrier Concentration n_o (cm^{-3})	Resistivity (Ω.cm)	Mobility $cm^2\ V^{-1}\ S^{-1}$	Carrier Type
ZnO (undoped)	4.69×10^{14}	2.62×10^{2}	50.9	n
PNZO (0.25)	2.34×10^{18}	19.1	0.14	p
PNZO (0.50)	2.73×10^{18}	18.1	2.42	p
PNZO (0.75)	4.48×10^{18}	9.6	5.58	p
PNZO (1.00)	7.25×10^{17}	17.8	4.48	p
PNZO (1.25)	5.34×10^{17}	21.5	3.46	p
PNZO (0.75) nanopencils	5.40×10^{18}	26.8	0.52	p

Table 2. The electrical properties and stability of PNZO (0.75 at%) seed layers and PNZO (0.75 at%) nanopencils examined after a time period of five months.

Sample	Carrier Concentration n_o (cm^{-3})	Resistivity (Ω.cm)	Mobility $cm^2\ V^{-1}\ S^{-1}$	Carrier Type
PNZO (0.75)	2.58×10^{17}	15.6	1.55	p
PNZO (0.75) nanopencils	2.75×10^{18}	27.9	0.86	p

atoms during modified aqueous chemical growth process and (c) the final product of as-grown PNZO nanopencils after 5 h of modified ACG process.

3.2. Electrical studies

The electrical properties of as-deposited PNZO seed layers and nanopencils were investigated by Hall-effect measurement in van der Pauw configuration at room temperature. Table 1 shows the electrical properties of undoped ZnO films, PNZO (0.25–1.25 at%) seed layers and PNZO (0.75) nanopencils. Undoped ZnO shows n-type characteristics with electron carrier concentration value of $4.69\times10^{14}\ cm^{-3}$ and higher resistivity value of $2.62\times10^{2}\ \Omega$.cm and. Upon doping P and N dual acceptor elements, all the samples are found to exhibit p-type conductivity, which indicates successful realization of p-type ZnO by dual acceptor doping of phosphorous and nitrogen. When the doping concentration of P and N is varied from 0.25 at% to 0.75 at%, a reduction in electrical resistivity is observed. The lowest resistivity obtained is $9.6\ \Omega$.cm with carrier concentration of $4.48\times10^{18}\ cm^{-3}$ for PNZO (0.75) seed layers. The resistivity value increases, when the P-N doping concentration is increased further beyond 0.75 at%. Phonon scattering and ionized impurity scattering takes place at higher doping concentration. This leads to increase in resistivity beyond optimum doping concentration of P and N (0.75 at%). The optimum as-deposited PNZO (0.75) seed layers were used for further surface modification in the form of one- dimensional nanopencils by the ACG process. In general, ZnO possesses a number of intrinsic defects with different ionization energies such as O vacancy (V_O), Zn vacancy (V_{Zn}), Zn interstitial (Zn_i), O interstitial (O_i) and antisite Zn (Zn_O). Among these defects, oxygen vacancy (V_O), zinc interstitial (Zn_i) and hydrogen incorporation are considered to be native electron donor defects. On the other hand, zinc vacancy (V_{zn}) and oxygen interstitial (O_i) are considered to be acceptor-like defects [23]. Since zinc nitrate is used as a precursor source, there is a greater possibility that electron donor defects such as V_O, Zn_i and Zn_O can be produced during the ACG process. This may lead to compensating the p-type behavior during nanopencil growth of PNZO (0.75). However, as P and N are intentionally doped in the ACG process (as discussed in the experimental section), the self-compensation effect is controlled effectively and successful growth of p-type ZnO nanopencils has been realized. The reason is well attributed to the contribution of more acceptor defects (O_i) which are formed during the ACG process. The as-grown PNZO nanopencils exhibit higher hole concentration of $5.40\times10^{18}\ cm^{-3}$ and the resistivity value is increased to $26.8\ \Omega$.cm in comparison with seed layers. The prominent reason for increase in resistivity of PNZO nanopencils is due to weak bonding between neighboring atoms and scattering of electron which occurs from the surface of the PNZO nanopencils [24]. To verify the stability of p-type conductivity in PNZO samples, the electrical measurements are performed several times and nearly the same results are obtained. The samples are preserved in ordinary silica gel desiccators and the ageing effects are investigated after a time period of five months. Table 2 shows the electrical properties PNZO (0.75) seed layers and PNZO (0.75) nanopencils after a period of five months. The preserved samples retain the p-type characteristics with subtle variation in carrier concentration and resistivity.

It is mandatory to understand the formation mechanism for obtained p-type ZnO using P and N as dopant sources. The relation between concentration of defects in ZnO and its formation energy based on the density functional theory can be expressed by the following equations [25]

$$c = N_{\text{sites}} \exp\left(-E_f/K_B T\right) \tag{1}$$

where N denotes the number of sites the defect can be incorporated on, K_B is the Boltzmann constant, E_f is the formation energy of the defects and T is the temperature. The above equation reveals that when the formation energy of the defects is high the defects in ZnO are unlikely to form and the equilibrium concentration is low. Based on *ab initio*

theoretical predications, Tain and Zhao performed a detailed study for the formation of p-type ZnO using phosphorous and nitrogen [26]. It is revealed that upon dual acceptor doping of P and N in ZnO, passive defects complex P_{Zn}-$3N_O$ may form in which the phosphorous substitutes Zn site and three nitrogen atoms replace nearest neighbor O atoms. Hybridizations between p-states of P:N dopant atoms and d-state of Zn atoms takes place by p-d coupling mechanism. Thus, P_{Zn}-$3N_O$ complex may form an additional fully occupied band above the valence band maximum (VBM). When additional N atoms were added, it formed P_{Zn}-$4N_O$ complex with low ionization energy of 271 meV above the VBM of ZnO. This P_{Zn}-$4N_O$ complex is reduced to 115 meV from the impurity band of the P_{Zn}-$3N_O$ complex. Theoretical calculations also reveal the formation energy of P_{Zn}-$4N_O$ complex in Zn-rich condition is −1.28 eV, which is 18.87 eV lower than that of O-rich condition [26]. These characteristics result in successful realization of p-type ZnO using P and N as a dopant sources for ZnO.

3.3. Structural studies

Figure 4(a) shows the XRD patterns of undoped ZnO films and PNZO (0.25–1.25 at%) seed layers. All the XRD patterns exactly match with JCPDS 75-0576 and exhibit hexagonal wurtzite structure with a = 0.3242 nm and c = 0.5194 nm. High intense (002) peaks are observed for all the samples with respect to other peaks such as (101) and (103). This indicates that (002) plane possesses lower surface free energy than other planes [27]. Absence of secondary phases indicates that P and N doping elements did not alter the wurtzite structure of ZnO. At up to 0.75 at% of P:N doping concentration in the ZnO, the crystalline nature of the films is high, evident from the sharp (002) peaks. When the P and N doping concentration is increased beyond 0.75 at%, the crystalline nature of the films begins to degrade. This is because higher doping concentration may lead to segregation of ions in the grain boundaries which makes the film crystallinity deteriorate [28]. XRD studies reveal that the optimum value of the P and N doping concentration is 0.75 at% (PNZO (0.75)). Figure 4(b) shows the XRD pattern of the grown PNZO (0.75) nanopencils by the ACG process. The XRD pattern of PNZO (0.75) nanopencils shows an increase in intensity of the peaks and hence shows an improved crystallinity over the PNZO (0.75) seed layers. The increase in peak height of (002) plane shows that PNZO nanopencils possess a preferential growth rate along c-axis [29]. During the nanowire growth of PNZO (0.75) seed layers, Zn–O bond stretches along c-axis and contracts perpendicularly to c-axis. Due to this effect, the atoms along the nanowire surface tend to change their original position when compared to seed layers. This change results in relaxation of in-built strain of PNZO seed layers, as a result of which the crystallinity increases for the vertically aligned PNZO nanowires. The average crystallite size is calculated from Scherrer's formula [30] and is found to vary from 49 nm to 42 nm with increase in doping concentration of P and N ions in ZnO films, whereas it is 64 nm for the as-grown nanowires. For the wurtzite structure of ZnO, the relation between interplanar distance (d_{hkl}), lattice parameters and Miller indices (hkl) can be expressed as [31]

$$\frac{1}{d^2_{(hkl)}} = \frac{4}{3}\left[\frac{h^2 + hk + k^2}{a^2}\right] + \frac{l^2}{c^2} \tag{2}$$

It is calculated that lattice constant 'c' for all PNZO seed layers and nanopencils is larger than the bulk ZnO. This indicates the presence of residual tensile strain for P and N dual acceptor doped ZnO samples. The average uniform strain ε_{zz} has been estimated from the lattice parameters using the following expression [31]

$$\varepsilon_{ZZ} = \frac{c_{film} - c_{bulk}}{c_{bulk}} \times 100 \tag{3}$$

where c_{bulk} refers to unstrained lattice parameter for bulk ZnO with value of 0.5194 nm (JCPDS no: 75-0576) and c_{film} refers to strain which occurs after dual acceptor doping of P and N atoms in ZnO. The residual stress in the films is composed of thermal stress and intrinsic stress. However, in the present study the effect of thermal stress it is assumed to be negligible since the deposition temperature is maintained constant for all the prepared samples. The effect of residual stress along (002) plane for PNZO seed layers and nanopencils is calculated using biaxial strain model [31]

$$\sigma_{film} = \frac{2C_{13}^2 - C_{33}(C_{11} - C_{12})}{C_{13}} \cdot \varepsilon_{ZZ} \tag{4}$$

where $C_{11} = 209.7$ GPa, $C_{12} = 121.1$ GPa, $C_{13} = 105.1$ GPa, and $C_{33} = 210.9$ GPa are the elastic stiffness constants of bulk ZnO. Table 3 shows the calculated lattice constant 'c', position of (002) peak, average crystallite size, strain and stress for undoped ZnO, PNZO (0.25–1.25 at%) seed layers and PNZO (0.75 at%) nanopencils. The negative value of calculated stress illustrates the presence of compressive stress along the (002) plane and the values are found to be higher for all P and N doped ZnO samples in comparison with undoped ZnO. The reason is well attributed to higher atomic radii doping elements such as P and N ions in ZnO lattices. Upon increasing the P and N doping concentration from 0.25 at% to 0.75 at% the value of stress decreases from −5.3720 GPa to −4.4364 GPa and these values increase at higher doping concentration. Segregation of more ions in the grain boundaries of PNZO seed layers at higher doping concentration beyond P:N (0.75 at%) is considered to be the primary reason for the increase in compressive stress along (002) planes. Figure 4(c) shows the deviation in the position of 2(θ) peaks along the (002) planes which confirms the presence of compressive stress upon doping P and N ions in ZnO. By comparing PNZO (0.75) seed layers and nanopencils, the latter show an increased stress value of −5.4754 GPa. It can be perceived that the doping effect involved in m-ACG process results in higher stress value for PNZO (0.75) nanopencils. It is also revealed, though in-built strain relaxes for PNZO (0.75) during ACG process and promotes one-dimensional nanostructures, that the doping effect of additional P and N atoms in the ACG process contributes higher stress formation which consecutively results in sharp edged nanowires. Hence,

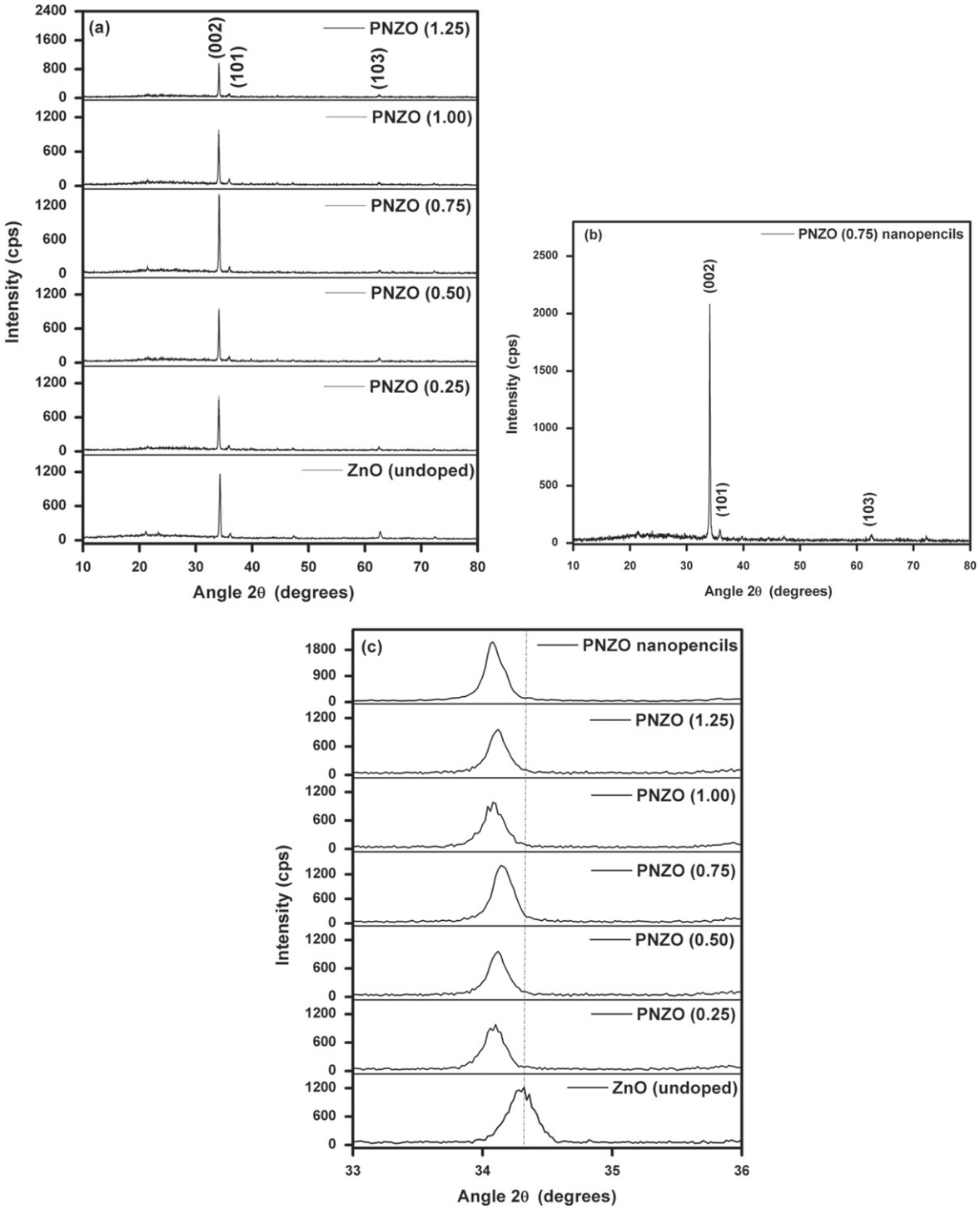

Figure 4. XRD patterns of (a) undoped ZnO films and PNZO (0.25–1.25 at%) seed layers (b) PNZO (0.75 at%) nanopencils and (c) the deviation in the position of 2(θ) peaks along the (002) planes.

the structural and morphological analysis exactly correlates for the reason behind the growth of pencil-like nanowires.

3.4. Optical studies

Figure 5 shows the optical transmission and reflectance spectra of (a) PNZO 0.25–1.25 at% and (b) PNZO (0.75 at%) pencil-like nanowires. The average transmittance of PNZO seed layers is 65%, while the PNZO nanopencils exhibit 45% transmittance. The decrease in transmittance of pencil-like PNZO nanowires can be attributed to the increase in thickness and the scattering of light on the surface owing to the increase in surface roughness of the nanowire samples. The absorption coefficient is evaluated using the following relation [15]

$$T = (1 - R)\exp(-\alpha t), \tag{5}$$

where T is the transmittance, R is the reflectance and t is the film thickness. PNZO films are considered as a material

Table 3. Calculated Lattice constants, 2θ position, crystallite size, strain and stress of undoped ZnO, PNZO (0.25–1.25 at%) seed layers and PNZO (0.75 at%) nanopencils.

Sample	C (Å)	2θ (degree)	Crystallite size (nm)	Strain	Stress (GPa)	Band gap (eV)
ZnO (undoped)	5.2221	34.31	37	0.5390	−2.4449	—
PNZO (0.25)	5.2559	34.09	42	1.1917	−5.3720	3.254
PNZO (0.50)	5.2514	34.11	44	1.1051	−5.0128	3.237
PNZO (0.75)	5.2448	34.15	49	0.9780	−4.4364	3.209
PNZO (1.00)	5.2535	34.09	43	1.1359	−5.1525	3.195
PNZO (1.25)	5.2559	34.08	42	1.1917	−5.4023	3.139
PNZO (0.75) nanopencils	5.2567	34.07	64	1.1207	−5.4754	3.212

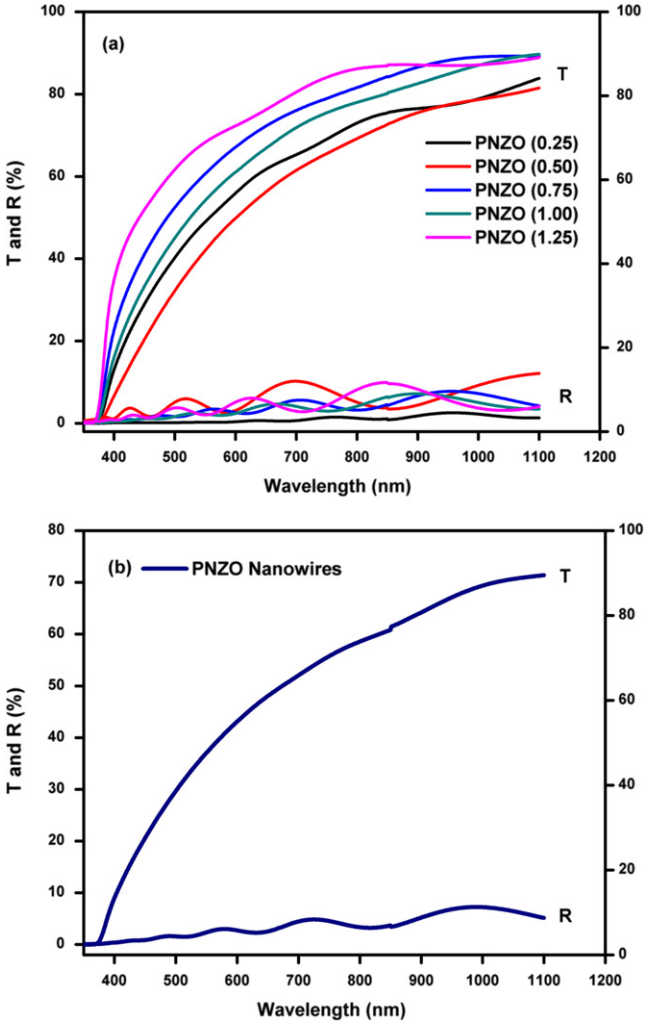

Figure 5. Optical transmission and reflectance spectra of (a) PNZO (0.25–1.25 at%) seed layers and (b) PNZO (0.75 at%) nanopencils.

having direct band gap and the band gap energy can be calculated using the following equation [15]

$$\alpha h\nu = B\left(h\nu - E_g\right)^{1/2}, \tag{6}$$

where E_g is the optical band gap, $h\nu$ is the incident photon energy and B is a constant. Figure 6 shows the $(\alpha h\nu)^2$ versus $h\nu$ plot for PNZO 0.25–1.25 at% and PNZO (0.75 at%) pencil-like nanowires. The linear portion of the graph is extrapolated in order to find the optical band gap of the prepared

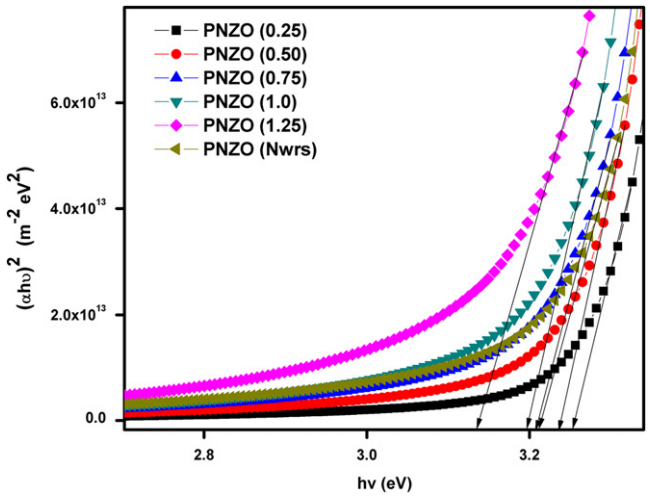

Figure 6. $(\alpha h\nu)^2$ versus $h\nu$ plot of PNZO (0.25–1.25 at%) seed layers and PNZO (0.75 at%) nanopencils.

samples. It is observed that when the P-N doping concentration increases from 0.25–1.25 at% the band gap decreases. The band gap was found to exhibit red shift with values decreased from 3.254 eV to 3.139 eV. This band gap narrowing effect in p-type ZnO can be explained by considering the atomic wave function characteristics of the band edge states in ZnO [32]. The conduction band edge (CBE) of ZnO consists of zinc (Zn) 4s states and oxygen (O) 3s and 3p states. The valence band edge (VBE) is dominated by (O) 2p states, with only few contributions from (Zn) 3d states. This helps in narrowing the band gap of ZnO by doping appropriate elements in O-site with dopants possessing p-state atomic orbital energy different from oxygen. In the present study, by dual acceptor P and N doping the optical band gap was found to be narrowed from 3.254 eV to 3.139 eV. It is also observed that PNZO (0.75) nanowires have a band gap of 3.212 eV, whose value is nearly the same as that of PNZO (0.75) seed layers (3.209 eV). By theoretical observation [32] a coupling mechanism is proposed between p-states of the doping elements (phosphorous and nitrogen) and d-states of zinc which may result in formation of a defect band just above the valence band maximum (VBM). This proposed p–d coupling exchange interaction plays the key role for the reduction of band gap of ZnO [33]. Table 3 shows the calculated band gap values of PNZO (0.25–1.25 at%) seed layers and PNZO (0.75 at%) nanopencils.

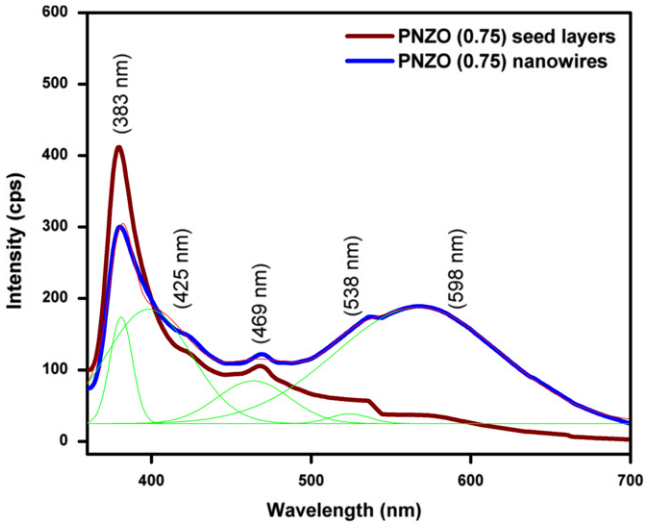

Figure 7. PL spectrum of PNZO (0.25–1.25 at%) seed layers and (b) PNZO (0.75 at%) nanopencils.

3.5. Photoluminescence studies

Figure 7 shows the PL emission properties of PNZO seed layers and PNZO pencil-like nanowires. It is observed that both PNZO seed layers and nanopencils exhibit strong UV emission at 383 nm. The presence of UV emission is one of the key characteristics of ZnO and it is attributed to band edge transition or exciton combination [34]. It is also observed that emissions in the visible range are strongly enhanced for the vertically aligned PNZO nanopencils after the ACG process. The broad emission in the visible region is plotted with Gaussian function fitting in order to study the violet (425 nm), blue (469 nm), green (538 nm) and yellow (598 nm) emission characteristics. These visible emissions in ZnO arise due to the presence of native donor and acceptor defects. A summarized reason for all the defects induced visible emission in ZnO with graphical representation based on the full potential linear muffin-tin orbital method can be found in our earlier reports [35]. The observed violet emission at 425 nm is due to transition energy from Zn_i to valence band [36]. Recombination between zinc interstitial (Zn_i) energy level to zinc vacancy (V_{Zn}) energy level contributes blue emission at 469 nm [37]. Intrinsic donor defects such as oxygen vacancies (V_o) contribute to green emission [38]. Yellow emission at 598 nm is attributed to the presence of oxygen interstitials (O_i) that act as acceptor-like defects. The presence of yellow emission is one of the common characteristics for ZnO nanostructures grown by aqueous chemical growth process. It is perceived that a greater number of acceptor-like defects (O_i) were formed during PNZO nanopencil growth, that resist against self-compensation effect and result in p-type characteristics of the grown nanopencils. Thus, by modified ACG process stable p-type ZnO nanopencils were successfully realized which also comprises broad emission characteristics in the visible region (400 nm to 700 nm) of the spectrum.

4. Conclusion

To summarize, a stable P and N dual acceptor doped p-ZnO has been realized by spray pyrolysis method. The p-type characteristic of the prepared samples was found to be stable by investigating its ageing effect for a time period of five months. The optimum dual acceptor doping concentration of P and N is found to be 0.75 at%, which is later used as seed layers in the ACG process in order to grow one-dimensional nanostructure. It is revealed that, after the ACG process, the grown nanostructures possess pencil-like morphology. From this investigation it is proposed that pencil like growth of ZnO is due to external stress caused by P and N in the ACG process, which results in sharp edges for the PNZO nanostructures. From the luminescence spectra analysis, it is observed that more acceptor-like defects (O_i) were formed during the ACG process which promotes broad emission in the visible region (400 nm to 700 nm) and also helps in sustaining stable p-type behavior for the grown PNZO nanopencils.

References

[1] Djurisic A B 2010 *Prog. Quant. Electron* **34** 191
[2] Huang M H, Mao S, Feick H, Yan H, Wu Y, Kind H, Weber E, Russo R and Yang P 2001 *Science* **292** 1897
[3] Law M, Greenel L E, Johnson J C, Saykally R and Yang P 2005 *Nat. Mater.* **4** 455
[4] Klingshirn C 2007 *Phys. Status Solidi* b **244** 3027
[5] Zhang Y Z, Lu J G, Ye Z Z, He H P, Zhu L P, Zhao B H and Wang L 2008 *Appl. Surf. Sci.* **254** 1993
[6] Pan X H, Jiang J, Zeng Y J, He H P, Zhu L P, Ye Z Z, Zhao B H and Pan X Q 2008 *J. Appl. Phys.* **103** 023708
[7] Tu M L, Su Y K and Ma C Y 2006 *J. Appl. Phys.* **100** 053705
[8] Fan J C, Sreekanth K M, Xie Z, Chang S L and Rao K V 2013 *Prog. Mater. Sci.* **58** 874
[9] Tang L D, Zhang Y, Yan X Q, Gu Y S, Qin Z and Yang Y 2008 *Appl. Surf. Sci.* **254** 4508
[10] Yamamoto T and Yoshid H K 2000 *J. Cryst. Growth* **214** 552
[11] Krtschil A, Dadgar A, Oleynik N, Bläsing J, Diez A and Krost A 2005 *Appl. Phys. Lett.* **87** 262105
[12] Sui Y R *et al* 2013 *Appl. Surf. Sci.* **287** 484
[13] Lu J G, Zhang Y Z, Ye Z Z, Zhu L P, Wang L, Zhao B H and Liang Q L 2006 *Appl. Phys. Lett.* **88** 222114
[14] Vlasenflin T H and Tanaka M 2007 *Solid State Commun.* **142** 292
[15] Amiruddin R and Kumar M C S 2014 *Ceram. Int.* **40** 11283
[16] Vayssieres L 2003 *Adv. Mater.* **15** 464
[17] Ahsanulhaq Q, Umar A and Hahn Y B 2007 *Nanotechnology* **18** 115603
[18] Baruah S and Dutta J 2009 *Sci. Technol. Adv. Mater.* **10** 013001
[19] Boppella R, Anjaneyulu K, Basak P and Manorama S V 2013 *J. Phys. Chem.* C **117** 4597
[20] Ghosh M, Karmakar D, Gadkari S C, Gupta S K, Basu S, Jha S N and Bhattacharyya D 2014 *J. Phys. Chem. Solids* **75** 543

[21] Zhou X, Xie Z X, Jiang Z Y, Kuang Q, Zhang S H, Xu T, Huang R B and Zheng L S 2005 *Chem. Commun.* **44** 5572
[22] Wang Z L 2005 *J. Mater. Chem.* **15** 1021
[23] Zhang S B, Wei S H and Zunger A 2001 *Phys. Rev.* B **63** 075205
[24] Lord A M, Maffeis T G, Walton A S, Kepaptsoglou D M, Ramasse Q M, Ward M B, Koble J and Wilks S P 2013 *Nanotechnology* **24** 435706
[25] Kohan A F, Ceder G, Morgan D and Walle C G V 2000 *Phys. Rev.* B **61** 15019
[26] Tian R Y and Zhao Y J 2009 *J. Appl. Phys.* **106** 043707
[27] Pedersen J D, Esposito H J and The K S 2011 *Nanoscale Res. Lett.* **6** 568
[28] Xu Z Q, Deng H, Li Y, Guo Q H and Li Y R 2006 *Mater. Res. Bull.* **41** 354
[29] Unalan H E, Hiralal P, Rupesinghe N, Dalal S, Milne W I and Amaratunga G A J 2008 *Nanotechnology* **19** 255608
[30] Patterson A L 1939 *Phys. Rev.* **56** 978
[31] Kumar V, Kumar V, Som S, Yousif A, Singh N, Ntwaeaborwa O M, Kapoor A and Swart H C 2014 *J. Colloid Interface Sci.* **428** 8
[32] Lu Y H, Russo S P and Feng Y P 2011 *Phys. Chem. Chem. Phys.* **13** 15973
[33] Ferhat M, Zaoui A and Ahuja R 2009 *Appl. Phys. Lett.* **94** 142502
[34] Reshchikova M A, Avrutin V, Izyumskaya N, Shimada R and Morkoc H 2007 *Physica* B **401** 374
[35] Amiruddin R and Kumar M C S 2014 *J. Lumin.* **155** 149
[36] Chen Y, Shao Y, Zhang X, Jia C, Su Y, Li Q, Liu L and Guo T 2011 *J. Nanosci. Nanotechnol.* **11** 1205
[37] Ahn H A, Kim Y Y, Kim D C, Mohanta S K and Cho H K 2009 *J. Appl. Phys.* **105** 013502
[38] Borseth T M, Svensson B G, Kuznetsov A Y, Klason P, Zhao Q X and Willander M 2006 *Appl. Phys. Lett.* **89** 262112